

Superlattice minibands—explicit formulae for band gaps and effective masses

G T Einevoll and P C Hemmer

Institutt for fysikk, Norges Tekniske Høgskole, Universitetet i Trondheim, N-7034 Trondheim, Norway

Received 19 June 1990, in final form 5 November 1990, accepted for publication 10 January 1991

Abstract. Explicit formulae for superlattice subband energies and effective masses in terms of the effective masses and layer widths of the constituent materials and the band offset are presented.

1. Introduction

With the development of special growth techniques such as molecular beam epitaxy (MBE) and metal organic vapour deposition (MOCVD), tailor-made submicrometre semiconductor heterostructures can now be designed. Binary superlattices, i.e. successive layers of two component materials, constitute important special cases. Their physical properties of foremost interest are the existence of narrow electron minibands, and it is clearly desirable to locate these minibands and to determine the effective masses associated with them.

Extensive calculations are necessary to determine these superlattice parameters from a microscopic theory. Our aim here is much more modest. We assume that we merely know the effective masses m_1 and m_2 of the component materials and the band-edge offset V_{off} . For given widths l_1 and l_2 of the layers, can one estimate the superlattice miniband structure? In particular, will the (band-edge) parallel and transverse effective masses be weighted averages of the two effective masses m_1 and m_2 , and if so, which averages?

We will, naturally, use effective mass theory, insisting throughout, however, on completely *explicit* formulae. This is achieved by a perturbative analysis of the exact effective mass condition for minibands. The explicit formulae allow one to see directly how the miniband parameters depend upon the layer widths, the effective masses of the components, the offset, and the miniband number. It goes without saying that the qualitative and quantitative insight one gains is important when designing superlattices for specific applications.

Results are given for conduction band (CB) superlattice minibands (based on a single-band effective mass theory). In section 2 the lower boundary of the miniband sequence is treated. Section 3 gives results for the gaps that open up at higher energies. In section 4 we discuss how strain may perturb the miniband structure. In the

final section 5 we give some concluding remarks and show a comparison between our explicit formulae for miniband energies and corresponding exact results (within the effective mass approximation) obtained numerically.

2. Principal miniband edge

Within the effective mass approximation, electronic motion is described by

$$-\frac{\hbar^2}{2} \nabla \frac{1}{m(x)} \nabla \psi + E^c(x) \psi = E \psi. \quad (1)$$

Here the effective mass $m(x)$ equals m_1 and m_2 (assumed isotropic), and the conduction-band edge $E^c(x)$ equals E_1^c and E_2^c , in materials 1 and 2, respectively. We have assumed the epitaxial layers to be a modulation in the x direction.

Insertion of

$$\psi(\mathbf{r}) = \exp(ik_y y + ik_z z) \phi(x) \quad (2)$$

yields the one-dimensional Schrödinger equation

$$-\frac{\hbar^2}{2} \frac{d}{dx} \frac{1}{m(x)} \frac{d\phi}{dx} + \left(E^c(x) + \frac{\hbar^2}{2m(x)} (k_y^2 + k_z^2) - E \right) \phi(x) = 0. \quad (3)$$

Previous controversies [1] about the correct ordering of the gradient operator and the space-dependent effective mass operator in the kinetic energy part of the effective mass Hamiltonian are now apparently settled [2, 3], with the result equation (1). (A possible exception occurs when the lattice constants of the two materials are different [4]. We postpone the discussion of this case to section 4.)

In equation (3) the variation of the effective potential

$$E_{\text{eff}} = E^c(x) + \frac{\hbar^2}{2m(x)}(k_y^2 + k_z^2) \quad (4)$$

has two contributions, one from the band offset and one from the difference in effective masses. Both are periodic modulations of the same type. The special case in which there is conduction-band alignment, i.e. when the offset

$$V_{\text{off}} = E_2^c - E_1^c \quad (5)$$

vanishes, has been denoted an effective mass superlattice, or a mass-modulation superlattice [5]. In the definition of the offset (equation (5)) we have arbitrarily assumed $E_2^c > E_1^c$ so that material 1 becomes the well material and material 2 the barrier material. The situation is sketched in figure 1.

With this simple effective potential it is straightforward to give an exact expression for the dispersion relation $E(k)$ of the system. The result is [6]

$$\begin{aligned} & \cos(q_1 l_1) \cos(q_2 l_2) \\ & - \frac{1}{2} \left(\frac{m_2 q_1}{m_1 q_2} + \frac{m_1 q_2}{m_2 q_1} \right) \sin(q_1 l_1) \sin(q_2 l_2) \\ & = \cos[k_x(l_1 + l_2)] \end{aligned} \quad (6)$$

where q_1 and q_2 are connected with the energy E through

$$E = E_1^c + \frac{\hbar^2(k_y^2 + k_z^2)}{2m_1} + \frac{\hbar^2}{2m_1} q_1^2. \quad (7)$$

and

$$E = E_2^c + \frac{\hbar^2(k_y^2 + k_z^2)}{2m_2} + \frac{\hbar^2}{2m_2} q_2^2. \quad (8)$$

The auxiliary variable q_2 is purely imaginary in the most interesting energy region $E_1^c < E < E_2^c$, ($k = 0$).

The difference between equations (8) and (7) connects q_1 and q_2 :

$$\frac{\hbar^2}{2} \left(\frac{q_1^2}{m_1} - \frac{q_2^2}{m_2} \right) = V_{\text{off}} + \frac{\hbar^2}{2} k_{\parallel}^2 \left(\frac{1}{m_2} - \frac{1}{m_1} \right) \quad (9)$$

with

$$k_{\parallel}^2 = k_y^2 + k_z^2.$$

At constant k_{\parallel} the right-hand side of (9)

$$V_{\text{off}} + \frac{\hbar^2}{2} k_{\parallel}^2 \left(\frac{1}{m_2} - \frac{1}{m_1} \right) \equiv V_{\text{off}}^{\text{eff}} \quad (10)$$

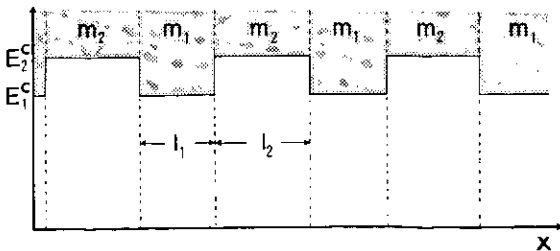


Figure 1. Profile of conduction band edge in the superlattice.

acts as an effective offset potential for transverse motion, i.e. motion perpendicular to the material interfaces.

Our main strategy is to use the offset V_{off} as a perturbation parameter. Also, k_{\parallel} is considered small. However, as discussed in the concluding remarks, the perturbation can be performed at finite k_{\parallel} , as long as the effective offset potential $V_{\text{off}}^{\text{eff}}$ is small.

The smallness of V_{off} is measured on the energy scale $\hbar^2/2m_i l_i^2$ in material i . Thus

$$V_{\text{off}} \ll \frac{\hbar^2}{2m_i l_i^2} \quad (i = 1, 2)$$

is assumed. This is important when the isolated quantum well limit $l_2 \rightarrow \infty$ is taken (see the concluding remarks).

For small offsets and for energies near the band edge we expand equation (6) in powers of q_1 and q_2 :

$$\begin{aligned} & 1 - \frac{1}{2} \left(\frac{l_1 q_1^2}{m_1} + \frac{l_2 q_2^2}{m_2} \right) (l_1 m_1 + l_2 m_2) + O(q_i^4) \\ & = \cos[k_x(l_1 + l_2)]. \end{aligned} \quad (11)$$

Eliminating q_1^2 and q_2^2 by means of equations (7) and (8), and expanding the right-hand side of (11) to second order of k_x , we obtain

$$\begin{aligned} E & = \frac{l_1}{l_1 + l_2} E_1^c + \frac{l_2}{l_1 + l_2} E_2^c + \frac{\hbar^2}{2} \frac{l_1 + l_2}{l_1 m_1 + l_2 m_2} k_x^2 \\ & + \frac{\hbar^2}{2} \left(\frac{l_1}{m_1} + \frac{l_2}{m_2} \right) \frac{k_{\parallel}^2}{l_1 + l_2}. \end{aligned} \quad (12)$$

The principal (lowest) CB edge E_0^c corresponds to $k = 0$, i.e.

$$E_0^c = E_1^c + \frac{l_2}{l_1 + l_2} V_{\text{off}}. \quad (13)$$

The quadratic terms in equation (12) yield the effective mass m_{\perp}^* for electronic motion parallel to the growth direction as

$$m_{\perp}^* = \frac{l_1}{l_1 + l_2} m_1 + \frac{l_2}{l_1 + l_2} m_2 \quad (14)$$

and the parallel effective mass m_{\parallel}^* via

$$\frac{1}{m_{\parallel}^*} = \frac{l_1}{l_1 + l_2} \frac{1}{m_1} + \frac{l_2}{l_1 + l_2} \frac{1}{m_2}. \quad (15)$$

Thus the transverse effective mass and the *inverse* parallel mass both arise as averages with the layer width fractions. This interesting difference implies the inequality

$$m_{\perp}^* \geq m_{\parallel}^*.$$

Equation (13) for the principal CB edge, and equations (14) and (15) for the corresponding band-edge effective masses, exemplify the type of explicit results we are aiming at. They are lowest-order results, however. In order to see how the effective masses depend on the offset we must go to the next order.

Carrying the expansion of equation (6) to fourth order in the quantities q_i , we generalize (11) to the

following expression

$$\begin{aligned}
 & -\frac{1}{2} \left(\frac{l_1 q_1^2}{m_1} + \frac{l_2 q_2^2}{m_2} \right) \left(l_1 m_1 + l_2 m_2 - \frac{q_1^2 l_1^2}{12} (l_1 m_1 + 2l_2 m_2) \right. \\
 & \quad \left. - \frac{q_2^2 l_2^2}{12} (l_2 m_2 + 2l_1 m_1) \right) \\
 & + \frac{l_1 l_2}{24 m_1 m_2} (l_1 m_1 + l_2 m_2)^2 q_1^2 q_2^2 \\
 & = -\frac{1}{2} (l_1 + l_2)^2 k_x^2. \tag{16}
 \end{aligned}$$

We have only kept terms up to second order in k_x . Equations (9) and (16) constitute two equations for q_1^2 and q_2^2 . Solving these perturbatively, we obtain the parabolic dispersion relation

$$E = E_0^c + \frac{\hbar^2 k_{\parallel}^2}{2m_{\parallel}^*} + \frac{\hbar^2 k_x^2}{2m_{\perp}^*} \tag{17}$$

with the band edge

$$E_0^c = E_1^c + \frac{l_2}{l_1 + l_2} V_{\text{off}} - \frac{l_1^2 l_2^2 (m_1 l_1 + m_2 l_2)}{6\hbar^2 (l_1 + l_2)^3} V_{\text{off}}^2. \tag{18}$$

The transverse effective mass m_{\perp}^* is now given by

$$m_{\perp}^* = \frac{m_1 l_1 + m_2 l_2}{l_1 + l_2} \left(1 + \frac{l_1^2 l_2^2 (m_2 - m_1)}{3\hbar^2 (l_1 + l_2)^2} V_{\text{off}} \right) \tag{19}$$

while the parallel effective mass m_{\parallel}^* is found to be

$$\begin{aligned}
 \frac{1}{m_{\parallel}^*} &= \frac{l_1}{l_1 + l_2} \frac{1}{m_1} + \frac{l_2}{l_1 + l_2} \frac{1}{m_2} \\
 & - \frac{l_1^2 l_2^2 (m_1 l_1 + m_2 l_2)}{3\hbar^2 (l_1 + l_2)^3} \left(\frac{1}{m_2} - \frac{1}{m_1} \right) V_{\text{off}}. \tag{20}
 \end{aligned}$$

With a heavier effective mass in the barrier material than in the well material, the resultant transverse effective mass will be heavier, and the parallel effective mass lighter, than the simple averages in equations (14) and (15) predict, and vice versa.

3. Higher minibands

For higher minibands we cannot work quite as explicitly as near the principal band edge, and we choose to perturb in the mass difference

$$\Delta m = m_2 - m_1$$

as well as in the offset V_{off} .

When Δm and V_{off} are both very small, then $q_1 \approx q_2$ by equation (9), and the exact dispersion relation (6) shows that the band gaps will be in the neighbourhood of $q_1 \approx q_2 \approx q_0$, where

$$q_0 = \frac{n\pi}{l_1 + l_2}. \tag{21}$$

Here the integer n is the gap number. The band edges

correspond to

$$k_x^c = \begin{cases} 0 & \text{(even } n) \\ \pi/(l_1 + l_2) & \text{(odd } n) \end{cases}. \tag{22}$$

We now expand in the deviations $\delta q_i = q_i - q_0$. From the energy relation (9) we find, to lowest order,

$$q_0 \left(\frac{\delta q_1}{m_1} - \frac{\delta q_2}{m_2} \right) = \hbar^{-2} V_{\text{off}} - \frac{\Delta m}{2m_1 m_2} q_0^2 - \frac{\Delta m}{2m_1 m_2} k_{\parallel}^2, \tag{23}$$

and the exact dispersion relation (6) yields, again to lowest order,

$$\begin{aligned}
 & (l_1 \delta q_1 + l_2 \delta q_2)^2 \\
 & = \frac{1}{8} m_1 m_2 G^2 \left(\frac{\Delta m}{m_1 m_2} + \frac{2V_{\text{off}}}{\hbar^2 q_0^2} - \frac{\Delta m}{m_1 m_2 q_0^2} k_{\parallel}^2 \right)^2 \\
 & + (k_x - k_x^c)^2 (l_1 + l_2)^2. \tag{24}
 \end{aligned}$$

We have used equation (23) and kept terms up to second order in $(k_x - k_x^c)$. The gap parameter

$$G = \left[1 - (-1)^n \cos \left(\frac{l_1 - l_2}{l_1 + l_2} n\pi \right) \right]^{1/2} \tag{25}$$

will play a crucial role, as we shall see later.

We proceed by solving (23) and (24) for δq_1 and inserting back in the energy relation (7). This yields for $k_{\parallel} = 0$, $k_x = k_x^c$ the miniband edges

$$\begin{aligned}
 E_n^{\pm} &= E_1^c + \frac{l_2}{l_1 + l_2} V_{\text{off}} + \frac{\hbar^2 n^2 \pi^2 / (l_1 + l_2)}{2(m_1 l_1 + m_2 l_2)} \\
 & \pm \frac{n\pi G}{2\sqrt{2}} \left| \frac{\hbar^2 \Delta m}{m_1 m_2 (l_1 + l_2)^2} + \frac{2V_{\text{off}}}{n^2 \pi^2} \right|. \tag{26}
 \end{aligned}$$

The n th gap width is twice the last term, i.e.

$$\Delta E_n = \frac{n\pi G}{\sqrt{2}} \left| \frac{\hbar^2 \Delta m}{m_1 m_2 (l_1 + l_2)^2} + \frac{2V_{\text{off}}}{n^2 \pi^2} \right|. \tag{27}$$

Note that the gap parameter G vanishes for certain width ratios ($n = 2$ and $l_1 = l_2$, for example), and hence the gap closes up (in this approximation). Seemingly non-systematic variations of minigap widths with increasing energy can be traced to the n dependence of the gap parameter. We also see that the influence of the offset, relative to the effective mass difference, is most important for the low minigaps.

By also including quadratic terms in k_{\parallel} and $(k_x - k_x^c)$, we find by the same procedure

$$E_n(\mathbf{k}) = E_n^{\pm} + \frac{\hbar^2 k_{\parallel}^2}{2m_{\parallel}^*} + \frac{\hbar^2 (k_x - k_x^c)^2}{2m_{\perp}^*} \tag{28}$$

with the effective masses

$$m_{\perp}^* = \pm \frac{G}{2\sqrt{2}\pi n} \left| \Delta m + \frac{V_{\text{off}}(m_1 + m_2)^2 (l_1 + l_2)^2}{2\hbar^2 n^2 \pi^2} \right| \tag{29}$$

and

$$\frac{1}{m_{\parallel}^*} = \frac{l_1}{l_1 + l_2} \frac{1}{m_1} + \frac{l_2}{l_1 + l_2} \frac{1}{m_2} \mp \eta \frac{G}{\sqrt{2}\pi n} \frac{\Delta m}{m_1 m_2} \tag{30}$$

where

$$\eta = \text{sign}\left(\Delta m + \frac{V_{\text{off}}(m_1 + m_2)^2(l_1 + l_2)^2}{2\hbar^2 n^2 \pi^2}\right). \quad (31)$$

In our perturbative treatment the parallel effective mass m_{\parallel}^* deviates little from the component material effective masses, while the transverse effective mass m_{\perp}^* can be arbitrarily small. Comparing equations (27) and (29) we see that the transverse effective mass at a miniband edge is proportional to the width of the adjacent gap:

$$m_{\perp}^* = \pm \frac{m_1 m_2 (l_1 + l_2)^2 \Delta E_n}{2\pi^2 \hbar^2 n^2}. \quad (32)$$

4. Influence of strain

When the lattice constants of the two materials are unequal, the preceding effective mass treatment must be modified [3, 4]. Although often the lattice constants of the two superlattice components are nearly equal, strained heterostructures have recently attracted attention because of possible applications and interesting physics [7]. The main effect from strain on CB states in superlattices is to shift the band-edge energies of the constituent materials to effectively change the band misalignment [8]. This effect will thus be incorporated in the value of V_{off} , and all results from the previous sections apply.

Another effect arises from the influence of a position-dependent lattice constant on the effective mass boundary conditions to use at material interfaces in strained superlattices. In [4] it was proposed to generalize the effective mass Schrödinger equation (1) for strained superlattices as follows:

$$-\frac{\hbar^2}{2} a^\delta \nabla \frac{1}{m(x)} a^{-2\delta} \nabla a^\delta \psi + E^c(x) \psi = E \psi \quad (33)$$

where $a(x)$ is the spatially varying lattice constant. It was shown, by comparison with exactly solvable test cases, that the appropriate value of δ is 0 or -1 , depending on the properties of the band edges, and it was proposed that $\delta = -1$ should be used for conduction band states.

The exact dispersion relation [4] corresponding to equation (33) is based on the following generalization of equation (6)

$$\begin{aligned} & \cos(l_1 q_1) \cos(l_2 q_2) \\ & - \frac{1}{2} \left(\frac{a_2^{2\delta} m_2 q_1}{a_1^{2\delta} m_1 q_2} + \frac{a_1^{2\delta} m_1 q_2}{a_2^{2\delta} m_2 q_1} \right) \sin(q_1 l_1) \sin(q_2 l_2) \\ & = \cos[k_x (l_1 + l_2)]. \end{aligned} \quad (34)$$

Here a_1 and a_2 are the lattice constants in the growth direction, after accommodation of strain, in materials 1 and 2, respectively. The variables q_1 and q_2 are still connected to the energy according to equations (7) and (8).

With minor modifications the previous expansions can be carried out and we merely quote the results.

For the *principal* miniband edge we find

$$E_0^c = E_1^c + \frac{l_2 a_2^{-2\delta}}{l_1 a_1^{-2\delta} + l_2 a_2^{-2\delta}} V_{\text{off}} \quad (35)$$

with the parallel and transverse effective masses given by

$$\frac{1}{m_{\parallel}^*} = \frac{l_1 a_1^{-2\delta}}{l_1 a_1^{-2\delta} + l_2 a_2^{-2\delta}} \frac{1}{m_1} + \frac{l_2 a_2^{-2\delta}}{l_1 a_1^{-2\delta} + l_2 a_2^{-2\delta}} \frac{1}{m_2} \quad (36)$$

and

$$m_{\perp}^* = \frac{l_1 a_2^{-2\delta} + l_2 a_2^{-2\delta}}{(l_1 + l_2)^2} \left(l_1 a_1^{2\delta} m_1 + l_2 a_2^{2\delta} m_2 \right). \quad (37)$$

For $\delta = 0$ (or $a_1 = a_2$, of course) this reduces to the previous results (equations (13), (14) and (15)). For $\delta = -1$, however, the effect of the unequal lattice constants is felt, and consists in a shift of the parallel (transverse) effective mass in the direction of the mass of the component with the largest (smallest) lattice constant.

For the higher minibands we find the following generalization of the band-edge expression (26):

$$\begin{aligned} E_n^\pm &= E_1^c + \frac{l_2}{l_1 + l_2} V_{\text{off}} + \frac{\hbar^2 n^2 \pi^2 / (l_1 + l_2)}{2(m_1 l_1 + m_2 l_2)} \\ &\pm \frac{\hbar^2}{2\sqrt{2}} \frac{n\pi G}{(l_1 + l_2)^2} \left| \frac{\Delta m}{m_1 m_2} + \frac{2(l_1 + l_2)^2}{\hbar^2 n^2 \pi^2} V_{\text{off}} \right. \\ &\left. + 16\delta \frac{\Delta a}{(m_1 + m_2)(a_1 + a_2)} \right| \end{aligned} \quad (38)$$

where we have also expanded (to first order) in the lattice constant difference

$$\Delta a = a_2 - a_1.$$

The transverse effective mass is still given by the (now modified) energy gap through equation (32), and the expression for the parallel effective mass in (30) (with η defined as the sign of the quantity between the absolute value markers in equation (38)) still applies.

Since the relative lattice-constant deviation is usually much smaller than the relative effective mass difference between the components, this effect of strain on the miniband structure is a minor one.

5. Concluding remarks

We have derived explicit expressions for the miniband structure and the associated transverse and parallel masses for superlattices. Several comments are appropriate:

(i) Since a quantum well can be considered as a limiting case of a superlattice when the barrier width $l_2 \rightarrow \infty$, we can treat (unstrained) shallow quantum wells in a similar way. We cannot take the $l_2 \rightarrow \infty$ limit in the final expressions for superlattices since, as noted in section 2, $V_{\text{off}} 2m_2 l_2^2 \hbar^{-2} \ll 1$ was assumed. Instead, we take the quantum well limit in the *exact* effective mass

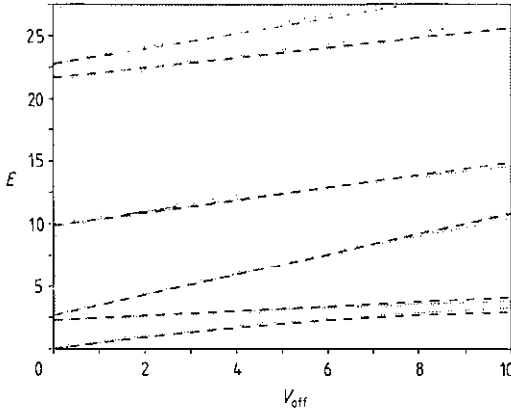


Figure 2. Superlattice miniband structure for $l_1 = l_2 = l$, $a_1 = a_2$, and $m_2 = 1.25 m_1$. Energies are given in units of $\hbar^2/(m_1 + m_2)l^2$. The full lines denote exact effective mass results, while the approximate results (equations (18) and (26)) are shown as broken lines. In this special case equation (26) yields a zero-width gap for $n = 2$.

formulae before proceeding to derive explicit results. For the lowest level one finds

$$E_0^c = E_2^c - \frac{m_2 l_1^2}{2\hbar^2} V_{\text{off}}^2 + \frac{m_2(3m_2 - m_1)l_1^4}{6\hbar^4} V_{\text{off}}^3 + \dots \quad (39)$$

with an associated parallel effective mass

$$m_{\parallel}^* = m_2 + m_2^2(m_1 - m_2)m_1^{-1}l_1^2\hbar^{-2}V_{\text{off}} + \dots \quad (40)$$

(ii) In order to test the quality of our analytic expressions we compare with numerical computations. Figure 2 shows how the miniband structure, derived from the exact effective mass expression (6), compares with the predictions of equations (18) and (26), for the case $l_1 = l_2$ and $m_2 = 1.25 m_1$, and for varying offset.

The figure shows that the analytic expressions work very well. The closing of the energy gap for even n (when $l_1 = l_2$) predicted by equation (26) is clearly seen for small offsets.

(iii) For experiments at constant k_{\parallel} both the offset V_{off} and the effective mass difference contribute to the effective offset potential $V_{\text{off}}^{\text{eff}}$ (equation (10)). For this case one can take over the explicit expressions (13), (18), (19), (26), (27), (29), (35), and (38) directly, replacing V_{off} by $V_{\text{off}}^{\text{eff}}$. Correspondingly, the validity of the perturbative approach is determined by the smallness of $V_{\text{off}}^{\text{eff}}$, not V_{off} and k_{\parallel} separately.

(iv) A final remark concerns the quality of the effective mass approach. In general it is expected to be an excellent approximation for energies that do not deviate too much from the bulk band edges. This can be (partially) checked on a microscopic model, and we refer to figure 4 of reference [3] for a comparison based on Krönig-Penney materials. As expected, the effective mass treatment gives a good representation of the first few minibands, but becomes inaccurate at higher energies.

In conclusion, we believe that when the effective mass approximation can be trusted, the closed-form expressions presented here are useful tools for estimations of superlattice miniband structures.

References

- [1] Morrow R A and Brownstein K R 1984 *Phys. Rev. B* **30** 678 and references therein
- [2] Einevoll G T and Hemmer P C 1988 *J. Phys. C: Solid State Phys.* **21** L1193
Galbraith I and Duggan G 1988 *Phys. Rev. B* **38** 10057
Thomsen J, Einevoll G T and Hemmer P C 1989 *Phys. Rev. B* **39** 12783
- [3] Einevoll G T, Hemmer P C and Thomsen J 1990 *Phys. Rev. B* **42** 3485
- [4] Einevoll G T 1990 *Phys. Rev. B* **42** 3497
- [5] Sasaki A 1984 *Phys. Rev. B* **30** 7016
- [6] Bastard G 1981 *Phys. Rev. B* **24** 5693
- [7] O'Reilly E P 1989 *Semicond. Sci. Technol.* **4** 121
- [8] See e.g. Smith D L and Mailhot C 1990 *Rev. Mod. Phys.* **62** 173